

Asymmetric Proton Transfer Catalysis by Stereocomplementary Old Yellow Enzymes for C=C Bond Isomerization Reaction

Marina S. Robescu, Laura Cendron, Arianna Bacchin, Karla Wagner, Tamara Reiter, Ignacy Janicki, Kemal Merusic, Maximilian Illek, Matteo Aleotti, Elisabetta Bergantino, and Mélanie Hall*



Cite This: *ACS Catal.* 2022, 12, 7396–7405



Read Online

ACCESS |



Metrics & More



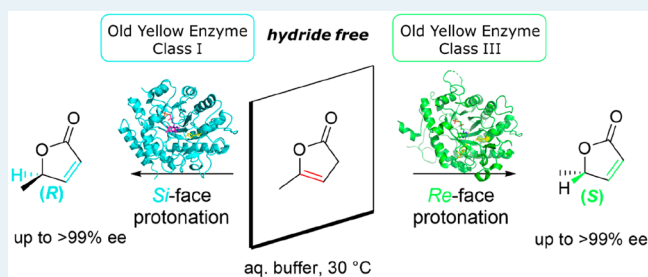
Article Recommendations



Supporting Information

ABSTRACT: Native and promiscuous catalytic activities of flavin-dependent Old Yellow Enzymes (OYEs) reported to date are initiated by the reduced flavin upon electron transfer. As a rare exception, the isomerization of a nonactivated C=C bond was shown to be hydride-independent with two nonstereoselective yeast OYEs. Here, we report the asymmetric isomerization of a prochiral model substrate, γ -methyl β,γ -butenolide, to the corresponding (*R*)- and (*S*)-enantiomers of the γ -methyl α,β -butenolide in up to >99% ee by two stereocomplementary OYEs of algal and fungal origin, respectively, which operate by asymmetric proton transfer. Mechanistic studies based on two newly solved crystal structures, along with soaking experiments and site-directed mutagenesis, support the crucial role of partially nonconserved tyrosine residues for the activity and stereoselectivity of both (*R*)- and (*S*)-isomerases. This study offers a unique view on the potential of flavoproteins in nonredox catalysis and provides hints for scouting olefin isomerases in likely stereodivergent classes of OYEs.

KEYWORDS: biocatalysis, catalytic promiscuity, flavoprotein, isomerization, Old Yellow Enzyme, stereodivergent



1. INTRODUCTION

Enzymes often catalyze reactions that differ from their physiological or natural activity—a principle coined catalytic promiscuity,^{1,2} and this feature has been largely exploited by chemists to design biosynthetic systems targeting specific needs.^{3–6} Although the resulting “new” chemical reaction differs from the natural one, in most cases, the same catalytic features are involved, and similar transition-state intermediates can be observed, as seen with members of the α/β -hydrolase fold superfamily.² Ene-reductases are flavoproteins from the Old Yellow Enzyme (OYE) family active in the asymmetric NAD(P)H dependent reduction of alkenes that are activated by the presence of an electron-withdrawing group on the C=C double bond. This group on the α -carbon lowers the electronic density of the double bond and favors attack on the β -carbon by the hydride.^{7–9} Nitro groups and nitroaromatics can also be reduced, and cases of reductive cleavage of nitrate esters have been reported.¹⁰ Recently, members of the OYE family were exploited for asymmetric carbocyclization via C–C-bond formation,¹¹ enantioselective dehalogenation of α -bromoesters,¹² carbonyl reduction in the presence of a photocatalyst,¹³ asymmetric radical dehalogenation/cyclization of α -chloroamides by photoexcitation,¹⁴ and photoinduced intermolecular radical hydroalkylation.^{15,16} These OYE-catalyzed non-natural reactions share in common the dependence on an external source of electrons to reduce the flavin coenzyme for initiation of the reaction.⁵ One notable exception

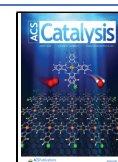
concerns the NAD(P)H-free hydride-independent isomerization of biomass-derived α -angelica lactone (γ -methyl β,γ -butenolide; **1**) to β -angelica lactone (γ -methyl α,β -butenolide; **2**), which we identified with OYE2 from *Saccharomyces cerevisiae*.¹⁷ The C=C bond isomerization reaction proceeded in a nonstereoselective manner, furnishing lactone **2** in racemic form. From a small panel of OYE homologues tested, significant activity could be observed only with OYE3 from *Saccharomyces cerevisiae* (82% sequence identity to OYE2).¹⁷

Enzymatic isomerization of C=C bonds is widespread in nature and relies on a diversity of proteins and, correspondingly, of mechanisms (Scheme 1). Several enzymes operate via acid–base catalysis with distinct catalytic residues. In the case of Δ^5 -3-ketosteroid isomerase,¹⁸ an aspartate shuttles a proton from the α - to the γ -position in the reaction with β,γ -unsaturated bicyclic ketones (Scheme 1A1). With 3-methylitaconate Δ -isomerase,¹⁹ a cysteine activated by a lysine carries out the intramolecular 1,3-proton transfer (Scheme 1A2). In the case of isopentenyl diphosphate isomerase type I (Scheme 1A3),²⁰ protonation of isopentenyl pyrophosphate by a

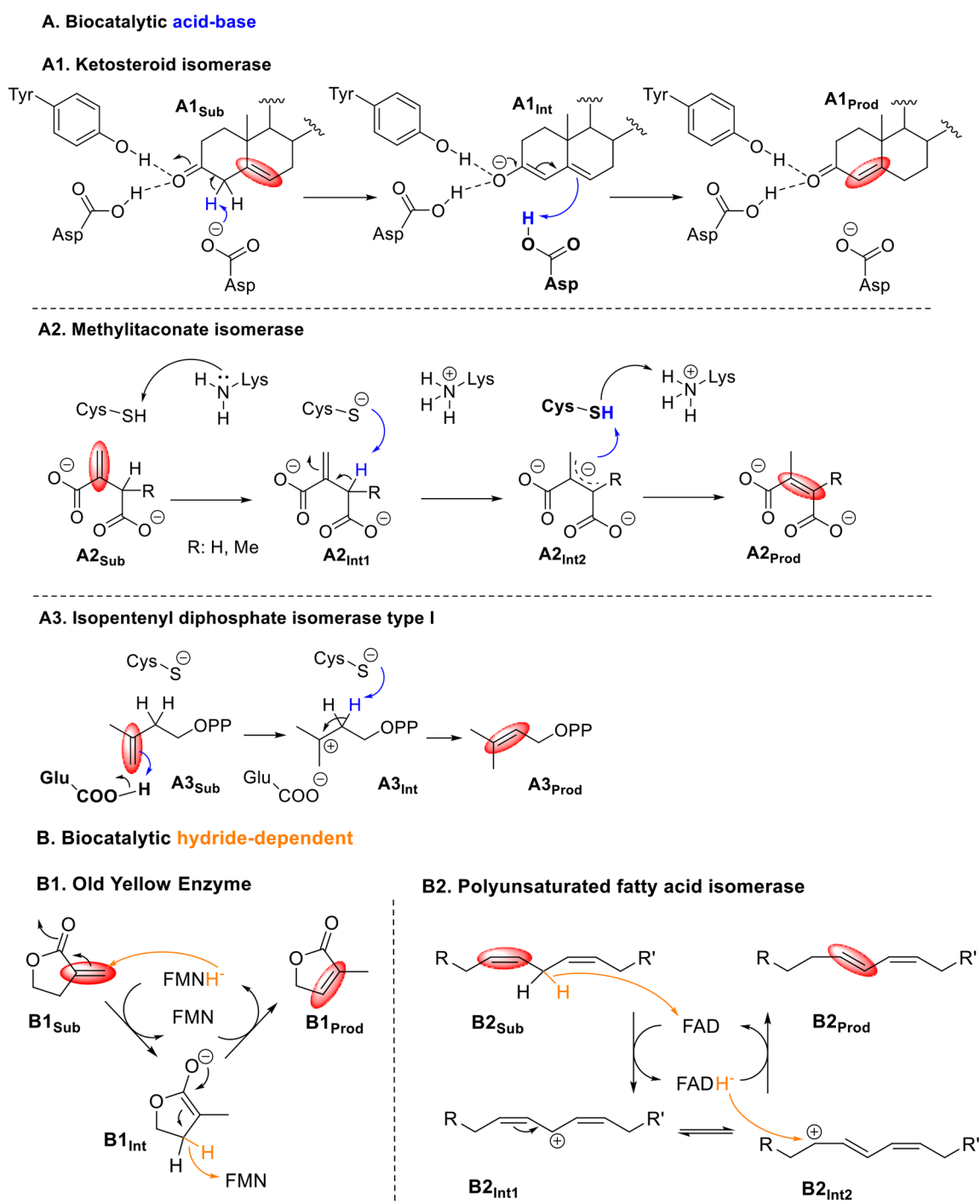
Received: March 4, 2022

Revised: May 20, 2022

Published: June 7, 2022



Scheme 1. Overview of Biocatalytic C=C Bond Isomerization Reactions Following A. Acid–Base Catalysis and B. the Hydride-Dependent Mechanism⁴²



⁴²Deprotonation-protonation sequence by A1: Δ^5 -3-ketosteroid isomerase;¹⁸ A2: 3-methylitaconate Δ -isomerase;¹⁹ protonation-deprotonation sequence by A3: isopentenyl diphosphate isomerase type I;²⁰ B1: hydride donation-abstracted *via* reduced flavin by Old Yellow Enzyme (external source of hydride required),²³ B2: hydride abstraction-donation *via* oxidized flavin by polyunsaturated fatty acid isomerase.²⁷ The following abbreviations apply for each sequence: Sub, substrate; Int, intermediate; Prod, product.

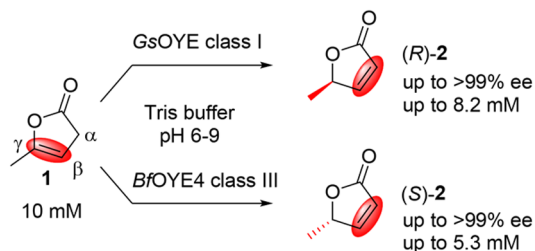
glutamic acid is followed by deprotonation by a cysteine-thiolate. Although flavin-dependent isopentenyl diphosphate isomerase type II also operates *via* acid–base catalysis, a reduced flavin is required to initiate the reaction. While the exact mechanism has not been fully elucidated, a direct catalytic role of the reduced flavin is likely.^{21,22} A reduced

flavin was also shown to be involved in the isomerization of 3-methylenedihydrofuran-2(3H)-one catalyzed by several OYE homologues (Scheme 1B1).²³ This unique mechanism, which is initiated by hydride transfer from the flavin onto the activated C=C bond, renders a formal intramolecular hydride shift and requires in theory only catalytic amounts of

NAD(P)H. Given the substitution pattern of all these substrates, no stereocenter is created through the isomerization reaction. Inspired by the case of ketosteroid isomerase, the Deng group developed an organocatalytic enantioselective isomerization protocol using cinchona alkaloids for proton transfer catalysis.²⁴ α -Angelica lactone and a range of β,γ -unsaturated butenolides were isomerized to the corresponding chiral γ -substituted α,β -unsaturated butenolides in up to 92% ee using a 10 mol % catalyst in dichloromethane at $-20\text{ }^{\circ}\text{C}$ for up to 60 h. Cooperative iminium-base catalysis by an aniline-functionalized cinchona alkaloid was later developed by the same group for the isomerization of β,γ -unsaturated cyclohex-3-en-1-ones to the corresponding conjugated enones.²⁵

Motivated by these works and aiming at the identification of stereoselective enzymes for asymmetric C=C bond isomerization reactions, we extended our screening efforts to underexplored sources of OYEs. During this campaign, promising candidates from photosynthetic extremophiles²⁶ as well as other organisms including Ascomycetes were selected for further characterization. The catalytic activity of two homologues with low sequence identity (21%, see Supporting Information, Table S2) from two different OYE classes was investigated in detail and revealed highly stereoselective and stereocomplementary behaviors in the isomerization of **1** (Scheme 2). Two new crystal structures were solved, and

Scheme 2. Stereoselective Hydride-Free Isomerization of α -Angelica Lactone (**1**) to β -Angelica Lactone (**2**) by Stereocomplementary OYE Homologues^a



^aGsOYE: OYE from *Galdieria sulphuraria*,²⁶ BfOYE4: OYE from *Botryotinia fuckeliana*.

analysis of the protein structures, along with soaking experiments and results from mutational study, revealed important aspects of this mechanism unique among OYEs, which is herein shown to proceed via asymmetric proton transfer catalysis in a stereodivergent manner.

2. RESULTS AND DISCUSSION

2.1. Protein Purification and Characterization.

In the frame of a genome mining-based campaign for the identification of OYE homologues from underexplored sources, enzyme candidates were discovered in photosynthetic extremophiles as well as Ascomycetes by using the sequences of OYE1 from *Saccharomyces pastorianus* and YqjM from *Bacillus subtilis* as templates. GsOYE²⁶ was identified in the polyextremophilic alga *Galdieria sulphuraria*, recombinantly overexpressed in *E. coli*, and purified to homogeneity. Based on protein primary structure, GsOYE was assigned to class I of the OYE family²⁸ (“classical OYEs” from plants and bacteria, see phylogenetic tree Figure S21) and showed C=C bond reducing activity on a large panel of activated alkenes.²⁶ The genome of the fungus *Botryotinia fuckeliana* contains four putative OYEs homologues that belong to different OYE classes.²⁹ The cells displayed strong reducing activity on cyclohex-2-en-1-one (**3**), and moderate activity was also detected with α -methylcinnamaldehyde.³⁰ Since the sequence of BfOYE4 (XP_001554780.1) is associated with members of class III²⁸ (“thermophilic-like OYEs”³¹), it was selected for further studies in order to enlarge the diversity of potential isomerases, noting that the only known OYE isomerases belong to class II.¹⁷ We obtained the corresponding gene by PCR amplification from the genomic DNA of *Botryotinia fuckeliana* B05.10. The protein bearing an N-terminal His₆-tag was heterologously expressed in *E. coli*, and despite low yields (7 mg/L), the enzyme could be obtained in soluble and pure form (see Supporting Information, Figure S2). The catalytic activity of the purified protein was verified on **3** in the presence of an excess of NADPH, and full conversion on 10 mM could be observed at pH 7 (Table 4). In aqueous Tris-HCl buffer (50 mM) at pH 8, the melting temperature measured by the Thermofluor assay reached 43 $^{\circ}\text{C}$. Although BfOYE4 is classified as a thermophilic-like OYE based on protein amino acid sequence similarities,⁷ its thermostability, as inferred from the protein melting temperature, remains modest and comparable with other enzymes from mesophilic organisms clustered into the thermophilic-like class and reported in the literature as nonthermostable OYEs (e.g., YqjM: $T_{\text{opt}} = 30\text{ }^{\circ}\text{C}$,³¹ XenA: T_{m} up to 37 $^{\circ}\text{C}$,³² OYERo2: stable up to 20 $^{\circ}\text{C}$,³³ RmER: $T_{\text{opt}} = 35\text{ }^{\circ}\text{C}$, and DrER: $T_{\text{opt}} = 30\text{ }^{\circ}\text{C}$ ³⁴).

2.2. Isomerization Reaction.

The isomerization of **1** was next investigated with both purified soluble proteins. In brief, 200–400 $\mu\text{g}/\text{mL}$ (~ 5 –10 μM , 0.05–0.1 mol %) enzyme was added to a solution of 10 mM **1** in Tris-HCl buffer (50 mM, pH 7–8) containing 2 vol% DMSO as the cosolvent, and the reaction mixture was incubated at 30 $^{\circ}\text{C}$ and 250 rpm overnight (Table 1). In the absence of NAD(P)H, **2** was detected as the sole product, and GC analysis of the extracted

Table 1. Influence of the pH on the Isomerization of **1 to **2** by OYEs^a**

enzyme	OYE2		GsOYE		GsOYE-P67K		BfOYE4		
	pH	rel activity ^b (%)	ee of 2 (%)	rel activity ^b (%)	ee of 2 (%)	rel activity ^b (%)	ee of 2 (%)	rel activity ^b (%)	ee of 2 (%)
	6	100	<i>rac</i>	9	>99 (R)	44	83 (R)	3	>99 (S)
	7	93	<i>rac</i>	57	84 (R)	125	81 (R)	41	98 (S)
	8	63	<i>rac</i>	61	77 (R)	76	34 (R)	61/74 ^c	92/93 ^c (S)
	8.5	n.t. ^d	n.a. ^e	n.t. ^d	n.a. ^e	n.t. ^d	n.a. ^e	60 ^c	88 (S)
	9	29	<i>rac</i>	32	16 (R)	n.t. ^d	n.a. ^e	47 ^c	80 (S)

^aReaction conditions: 10 mM **1**, 200 $\mu\text{g}/\text{mL}$ enzyme ($\sim 5\text{ } \mu\text{M}$), Tris-HCl (50 mM), 2 vol% DMSO, 30 $^{\circ}\text{C}$, overnight. ^bRelative activity based on the maximum amount of **2** obtained with OYE2 (set as 100% reference). ^c400 $\mu\text{g}/\text{mL}$ enzyme ($\sim 10\text{ } \mu\text{M}$). ^dn.t. not tested. ^en.a. not applicable.

reaction mixtures on chiral stationary phase revealed formation of the enantioenriched product in a stereodivergent manner (Scheme 2): GsOYE led to the formation of (*R*)-**2** in up to 84% ee, while (*S*)-**2** was obtained with BfOYE4 in excellent enantiopurity (up to 98% ee). At pH 7.5, 6.3 mM and 4.3 mM product, respectively, could be obtained using GsOYE and BfOYE4, respectively. In comparison, OYE2 generated 7.9 mM *rac*-**2** under the same reaction conditions (see Supporting Information, Table S8). The maximum amount of **2** formed with both enzymes was found dependent on the pH (*vide infra*); from 10 mM **1**, up to 8.2 mM (*R*)-**2** was obtained after 5 h of reaction time using 400 $\mu\text{g/mL}$ GsOYE at pH 7, and 5.3 mM (*S*)-**2** was obtained using 400 $\mu\text{g/mL}$ BfOYE4 at pH 8 (Tables 3 and 4).

The absolute configuration of enantioenriched **2** could be determined by measurement of the optical rotation of the product obtained using BfOYE4 ($[\alpha]_{\text{D}}^{20} = +35.6^\circ$ ($c = 0.34$, CHCl_3), see the Supporting Information), which coincides with values reported for the (*S*)-enantiomer.²⁴ The assignment of absolute configuration was later corroborated by soaking and X-ray experiments (*vide infra*). So far, a high level of activity in the isomerization reaction had only been observed with OYE2 (and to a lesser extent OYE3), but the enzyme was not stereoselective.¹⁷ OYE1 was tested this time, and strong catalytic activity with formation of the racemic product was observed (data not shown), an expected result given the high sequence identity between OYE1 and OYE2 (90%).

A detailed pH study was next conducted and revealed major differences between GsOYE, BfOYE4, and OYE2 (Table 1). Control experiments without enzyme did not lead to the formation of any product; only trace amounts of *rac*-**2** were found in all samples and taken into consideration for the calculation of conversions and ee values (see the Supporting Information). Noteworthy is that both GsOYE and BfOYE4 share a pH-independent activity profile in the reduction of **3** between pH 6–9 (see Supporting Information, Figure S11). While GsOYE and BfOYE4 both showed strongly diminished isomerization activity on **1** at pH 6, a stark pH-dependent stereoselectivity pattern was observed with GsOYE: at pH 6, (*R*)-**2** was formed in >99% ee, whereas max. 16% ee was obtained at pH 9. In contrast, (*S*)-**2** obtained with BfOYE4 could sustain significantly higher ee values, even at pH 9 (80% ee). OYE2 always furnished *rac*-**2** with the product level at the highest at pH 6. Also notable was the decrease in the product amount at basic pH values with all three enzymes, which was the least pronounced with BfOYE4. The substrate amount remained consistently low upon workup of the reactions at pH 8–9 (data not shown). The lability of **1** already at slightly basic pH has been shown to be responsible for low recoveries of this compound upon extraction, due to hydrolysis³⁵ and dimerization,³⁶ while **2** appears stable at up to pH 9.¹⁷ To better understand the erosion of the product enantiopurity with increasing pH values and to rule out racemization at the γ -C—which is not expected at this poorly activated/nonacidic position—a series of experiments were set up. First, isomerization of **1** was performed using GsOYE under standard conditions at pH 7 overnight. The pH was then either kept constant or adjusted to pH 8 or 9 for further incubation for 5 h. The ee of (*R*)-**2** was then measured and found to be strongly diminished after the change to higher pH values (from 90% at pH 7 to 80% at pH 8 and <5% at pH 9, data not shown), along with a lower amount of **2**. In contrast, the ee value remained constant at pH 9 when an enzyme heat deactivation step was

introduced prior to pH adjustment and further incubation, indicating that the drop in ee at basic pH was enzyme-mediated. Finally, adding fresh enzyme again and continuing incubation at pH 9 resulted in reduced ee and a lower amount of **2** (see Supporting Information, Table S5). Next, *rac*-**2** obtained by chemical synthesis was incubated in the presence of BfOYE4 at pH 9 for 5 h (Table 2), after which consumption

Table 2. “Reverse” Isomerization of *rac*-**2** at pH 9 with Selected Enzymes^a

enzyme	pH	consumption of <i>rac</i> - 2 [%] ^b	ee of 2 [%]
blank (no enzyme)	9	n.d. ^d	<i>rac</i>
BfOYE4	9	14	17 (<i>R</i>)
BfOYE4	7.5	9	<i>rac</i>
BfOYE4-Y78F	9	4	<i>rac</i>
GsOYE	9	22	16 (<i>S</i>)
GsOYE	7.5	10	4 (<i>S</i>)
GsOYE-Y179F	9	n.d. ^d	<i>rac</i>
GsOYE-Y66F	9	15	8 (<i>S</i>)
GsOYE-Y346F	9	24	9 (<i>S</i>)
OYE2	9	25	<i>rac</i>
OYE2 ^c	9	36	<i>rac</i>
OYE2	7.5	9	<i>rac</i>
OYE2-Y197F	9	3	<i>rac</i>

^aReaction conditions: 10 mM *rac*-**2** in buffer Tris-HCl (50 mM, pH 9 or 7.5), 2 vol% DMSO, 200 $\mu\text{g/mL}$ enzyme ($\sim 5 \mu\text{M}$), 30 °C, 5 h.

^bSubstrate consumption based on remaining *rac*-**2** compared to the initial amount present in the blank (blank, no consumption). ^c10 μM enzyme. ^dn.d. not detected.

of **2** could be observed, and an ee of 17% for the (*R*)-enantiomer of the remaining **2** was monitored. Thus, enantioenrichment by slow and (*S*)-enantioselective enzymatic reverse isomerization of **2** took place, following a kinetic resolution (E-value ~ 63). Due to the instability of **1** at such basic pH, only traces of **1** could be observed in the reverse isomerization. With GsOYE and at pH 9, consumption of **2** went hand in hand with its enrichment toward the (*S*)-enantiomer, confirming the (*R*)-enantiopreference of this enzyme. OYE2 showed again the strongest and non-enantioselective activity on *rac*-**2** (in that case, and using 10 μM OYE2, the corresponding formation of **1** could be detected, see Supporting Information, Figures S18). With all three enzymes, the extent of isomerization of *rac*-**2** was reduced at pH 7.5 compared to pH 9 (Table 2). Collectively, these data indicate that the apparent drop in product enantiopurity observed upon isomerization of **1** at basic pH (Table 1) is connected to an enantioselective consumption of **2** following its formation (“reverse” isomerization,²⁴ see Supporting Information, Scheme S1). Chemically analogous to the isomerization of **1** to **2**, the stereoselective allylic isomerization of the β,γ -unsaturated cyclic enone neopinone to the α,β -unsaturated analogue codeione was recently shown to be catalyzed by neopinone isomerase.^{37,38} Similar to our observations, neopinone isomerase was shown to be capable of catalyzing the isomerization of codeione “back” to neopinone. In theory, the isomerization toward formation of the α,β -unsaturated isomer (*i.e.*, neopinone to codeione and **1** to **2**) is favored^{39,40} due to the thermodynamic advantage of the conjugated system (e.g., **2** is 1 kcal/mol lower in energy than **1**⁴¹). With **2**, the instability of the resulting product **1** at basic pH and subsequent hydrolysis appears to provide a sufficient

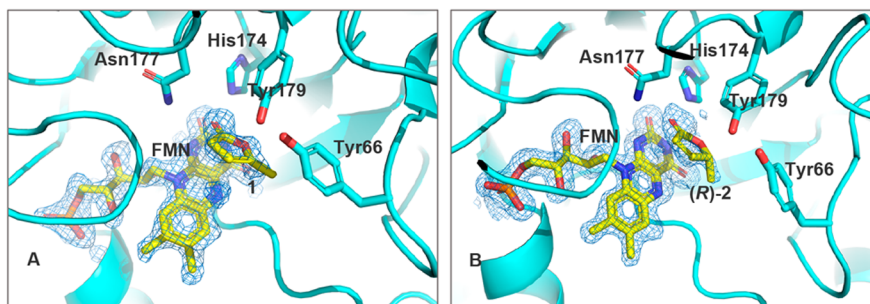


Figure 1. Time course crystallographic studies of GsOYE in complex with **1**. A) After 45 min, **1** is the main compound trapped in the enzyme active site, as demonstrated by composite omit maps. B) After 7 h, the enzymatic reaction product (*R*)-**2** is stacked on top of the FMN cofactor. Omit maps have been calculated in both cases by Phenix software and depict the electron density contoured at 3σ (for 2FOFC and FOFC maps, see Supporting Information, Figure S9).

thermodynamic drive for the isomerization to happen on the more stable α,β -unsaturated isomer, likely further driven by the tautomerism of the opened enol-isomer to the more stable keto-isomer (see Supporting Information, Scheme S1).⁴²

Given recent studies demonstrating the influence of light irradiation on the promiscuous activity of OYEs,^{14–16} the isomerization reaction of **1** was also performed in the dark with both GsOYE and OYE2 for 5 h. Upon workup, both amounts and ee values of product **2** were comparable to that obtained from the reaction performed under daylight, indicating a light-independent mechanism (see Supporting Information, Table S7). Finally, the effect of FMN alone (0.5 mM and 10 mM) was investigated on 10 mM **1** under standard reaction conditions in the absence of enzyme. After 5 h, no formation of **2** could be detected (data not shown), confirming the involvement of the enzyme in the reaction.

A small panel of β,γ -unsaturated acyclic compounds bearing an activating group (ester or nitrile) was tested, but under the tested reaction conditions, no product formation could be detected (see Supporting Information, Figure S22), indicating that a cyclic structure may be required for activity and/or that the relative positioning of the γ -C to the protonating residue is crucial for reactivity.

2.3. Crystal Structures and Soaking Experiments. The crystal structure of GsOYE was obtained in a previous study at a 1.45 Å resolution (PDB 6S0G).²⁶ Further experiments aiming at soaking compound **1** were conducted at pH 7 with already formed crystals with the incubation time ranging from 45 min to 7 h (see the Supporting Information). Crystals containing bound **1** were obtained after 45 min and revealed unambiguous substrate binding via H-bonding between the carbonyl oxygen atom and His174 and Asn177 (Figure 1A). Both hydroxy groups of Tyr66 (equivalent to Tyr83 in OYE2) and Tyr179 (equivalent to Tyr197 in OYE2) pointed toward the prochiral γ -C-atom of **1** (4.7 and 3.0 Å between the γ -C and the O-atom of the hydroxy group from Y66 and Y179, respectively). After 7 h of incubation of the crystals with **1**, an electron density mainly interpretable as product **2** and corresponding to the (*R*)-enantiomer was detected in the enzyme active site, indicating that the stereoselective isomerization had taken place within the crystal (Figure 1B). Binding was still mediated by His174 and Asn177, and the positioning of the methyl group at the now chiral γ -C, pointing toward the flavin, strongly hinted at protonation from Tyr179 on the *Si* face of the C=C bond of **1**. Tyr66, while also close to the γ -C-atom, appears in a better configuration for direct interaction with the hydroxy group of Tyr179 (2.7 Å between the two O-

atoms of both Tyr-OH groups), while in comparison, this distance is strongly increased in nonselective isomerase OYE2 (4.7 Å between Tyr83 and Tyr197, Figure 2), for which we also obtained a crystal structure (see Supporting Information, Figures S7–S10).

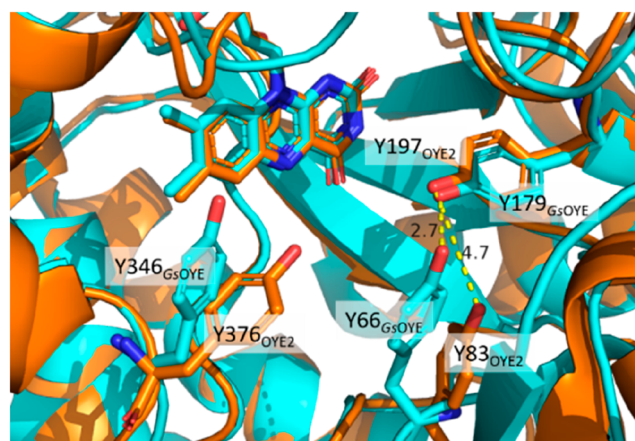


Figure 2. Structure overlay of (*R*)-isomerase GsOYE (cyan) and nonselective isomerase OYE2 (orange) with distances indicated between the tyrosine pairs (Å). Alignment of the α -carbon backbone obtained using PyMOL⁴⁴ (RMSD = 0.936 Å).

Polyunsaturated fatty acid isomerase (PAI) from *Propionibacterium acnes* is a flavin-dependent enzyme responsible for the irreversible isomerization of linoleic acid to 10,12-conjugated linoleic acid (10*E*, 12*Z*-isomer). The reaction proceeds through hydride shuffling and starts by abstraction of the hydride at C11 of the substrate by the N5-atom of FAD. After the allylic shift of the generated carbocation B2_{Int1}, the hydride attack occurs at C9 (B2_{Int2}), resulting in an intramolecular hydride shift and liberation of a diene as the final product (Scheme 1B2).^{27,43} Such a mechanism is not plausible in the isomerization of **1** by GsOYE. First, the crystal structure of GsOYE obtained after soaking with **1** shows the *Re* face of the C=C bond facing FMN, which is not compatible with the formation of (*R*)-**2** through hydride donation from the flavin. After extended soaking, an electron density corresponding to (*R*)-**2** was clearly identified in the active site, with the compound protonation site facing Tyr179, corresponding to protonation on the *Si* face of the C=C bond. Additionally, hydride abstraction from the α -C-atom of **1** is unlikely to happen given the acidity of the α -H, which should

preferentially be abstracted as proton. With PAI, hydride abstraction from the substrate is driven by the generation of an allylic carbocation stabilized by π -conjugation.²⁷ Collectively, these data indicate that stereoselective protonation of **1** in GsOYE occurs on the *Si* face of the substrate C=C bond through Tyr179.

To gain molecular insights into the stereodivergent behavior of GsOYE and BfOYE4, the crystal structure of BfOYE4 was elucidated (see Supporting Information, Figures S4–S6) and compared to the structure of GsOYE.²⁶ Soaking experiments with BfOYE4 were unfortunately unsuccessful. Despite overall good alignment of the α -carbon backbone (RMSD = 1.083 Å using PyMOL⁴⁴), major differences between GsOYE and BfOYE4 could be observed in the amino acids lining and building up the active site, including the presence of Tyr78 in the active site of BfOYE4 (equivalent to Asn27 in GsOYE) and the absence of Tyr66, which is one of the two tyrosine “gating” residues found in GsOYE (along with Tyr346) as well as in LeOPR1 (Tyr78 and Tyr358).⁴⁵ In BfOYE4, Tyr66 is replaced by Thr118 (see Supporting Information, Figure S1).

2.4. Mutational Studies. Based on the analysis of both crystal structures and soaking experiments with GsOYE, a few residues with a potential role in acid–base catalysis were targeted for mutations. A number of single variants were designed for GsOYE and BfOYE4, overexpressed in *E. coli*, purified (see Supporting Information), and tested in the native reduction reaction on **3** and the isomerization of **1** (Tables 3 and 4). With GsOYE, Thr25 was mutated to Cys, which is the equivalent residue in BfOYE4 and is conserved among thermophilic-like OYEs (class III).⁷ As seen in isopentenyl diphosphate isomerase type I,¹⁶ cysteine can potentially function as a base. No major impact was seen on the extent of isomerization, and the ee of (*R*)-**2** was barely affected (81% with T25C vs 90% at pH 7 with the wild-type). The data from soaking indicates that the binding mode of **1** orients α -C away from Thr25 (Figure 1). Residue Asn270 was selected owing to its relative proximity to the substrate, in particular of the nitrogen of the side chain amino group to α -C of **1** (5.9 Å). Mutation N270R did not impact the reductive activity but led to a severely reduced isomerization activity; however, this residue appears to be not involved in the stereoselectivity of the reaction (Table 3). Three tyrosine residues were next targeted due to their presence near the substrate: the two active site gating residues Tyr66 and Tyr346 as well as Tyr179. Mutation Y179F had the most detrimental effect on both

activity and stereoselectivity (5% of the activity of the wild-type and max. 32% ee for (*R*)-**2**). Y346F did not show much effect, except a slight reduction in ee of (*R*)-**2**, and with Y66F, although the extent of isomerization was dramatically reduced (2% of wild-type activity), the stereoselectivity was only moderately affected. Based on these data, Tyr179 appears to act in GsOYE as the stereoselective proton donor on the *Si* face of the C=C bond, as hinted from the soaking data, and in line with the protonating activity of this residue conserved in almost all OYE homologues in the bioreduction of C=C bonds.⁴⁶ Tyr66, which is in hydrogen-bonding distance of Tyr179–OH and further away from **1** (*vide supra*), is involved in catalysis but not in the direct protonation of the substrate. Instead, Tyr66 may be involved in proton relay by regenerating Tyr179 after proton donation to the substrate (Scheme 3A). This would explain the lower activity of Y66F due to slower regeneration of Tyr179 from the aqueous environment—and the conserved high ee values for the product obtained with this variant. A tyrosine network, although engaged in a dehydrogenation reaction, has also been observed in Δ^1 -ketosteroid dehydrogenase, with tyrosine residues appearing in different protonation states.⁴⁷ Since Pro67 is also present in LeOPR3 but is replaced by Lys in LeOPR1 with major impact on stereoselectivity in the reduction reaction,⁴⁸ GsOYE-P67K was constructed. Although the stereoselectivity was comparable to that of wild-type GsOYE in the isomerization of **1**, the single variant showed much stronger activity, in particular at pH 6–7 (Table 1). As in the case with the two homologues LeOPR1 and LeOPR3,³⁷ P67K may influence the position of Tyr66 by moving this residue closer to Tyr179, thereby supporting catalysis. The beneficial effect on activity was found even more pronounced by using more enzyme at pH 7 (see Supporting Information, Table S6 and Figures S12 and S13).

With BfOYE4, mutations C76A and C76T had no significant effect on the isomerization of **1** (Table 4). Two tyrosine residues were targeted next: Tyr235 (equivalent to GsOYE-Tyr179) and Tyr78, present at the bottom of the active site, with Tyr₇₈–OH pointing toward the inside of the binding pocket. Both mutations were highly detrimental to the isomerization reaction: with Y235F, no product formation could be detected, and with Y78F, diminished isomerization activity was monitored with a strongly reduced ee value for (*S*)-**2** (max. 25%). Regardless of the pH of the reaction, Y78F delivered consistently low ee values (Table 4). Finally, K157A had a major effect on the activity (19% of the wild-type activity), while the ee of (*S*)-**2** remained very high (91%). Without soaking data available, a combined role of these three residues in the mechanism of the isomerization can only be postulated: (i) Tyr235 as a tyrosinate deprotonates **1** at the α -C-atom; (ii) Lys157 reactivates Tyr235 through deprotonation (distance of 4.6 Å between the N-atom of the side chain Lys₁₅₇–NH₂ and the O-atom of Tyr₂₃₅–OH); (iii) Tyr78 stereoselectively reprotonates the enolate type intermediate on the *Re* face of the C=C bond, delivering the product (*S*)-**2** (Scheme 3B).

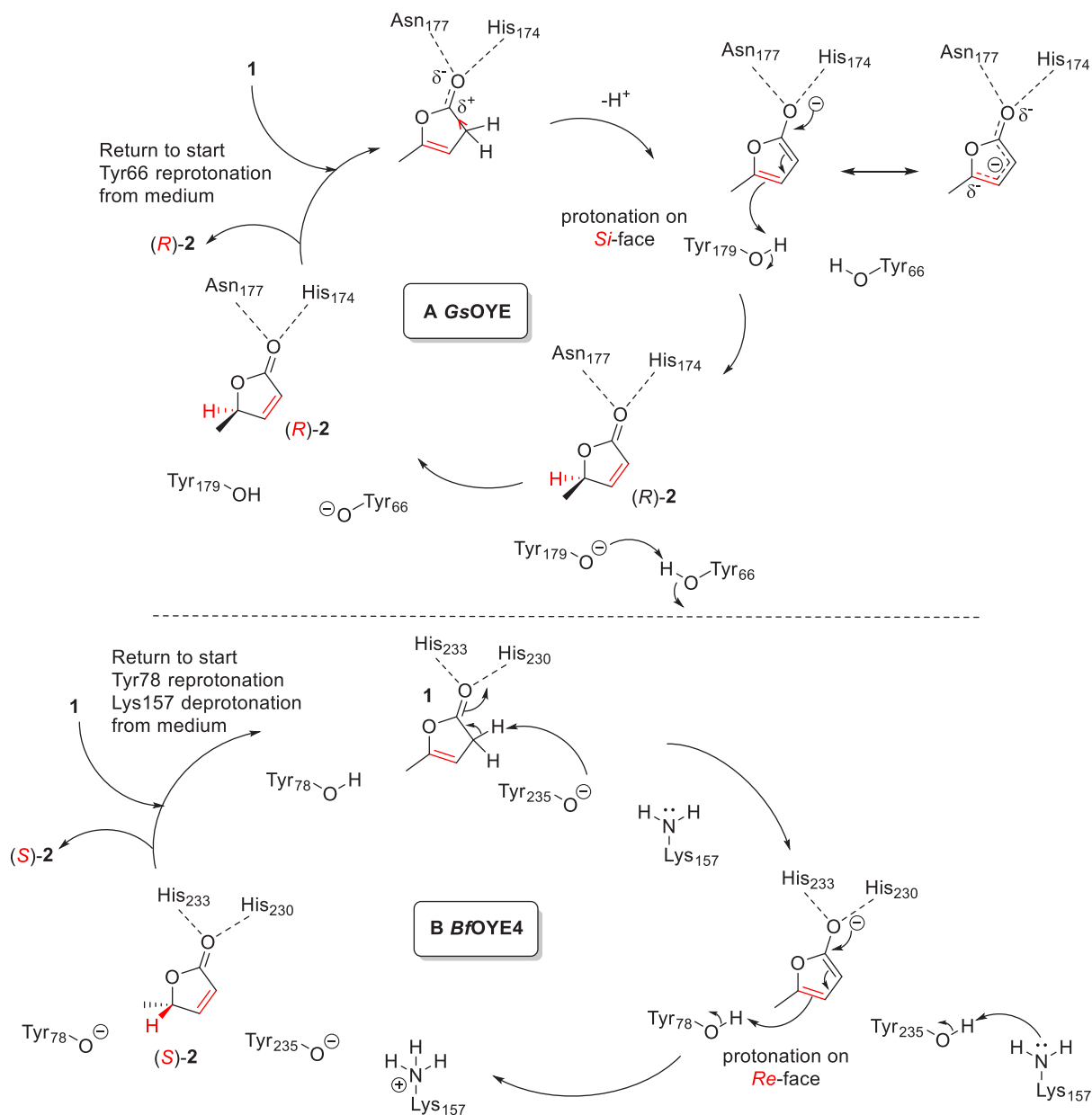
BfOYE4-Y78F and GsOYE-Y179F were also tested in the “reverse” isomerization of *rac*-**2** at pH 9 (Table 2), and in both cases, **2** remained racemic without significant consumption, confirming the crucial participation of both tyrosine residues in the mechanism of the asymmetric catalysis. With OYE2, mutation of Y197F resulted in a strong decrease in the isomerization of *rac*-**2** at pH 9 (from 25% consumption with the wild-type down to 3% with the single variant), while

Table 3. Activity of GsOYE Variants Compared to the Wild-Type in Isomerization of **1 to (*R*)-**2** and Reduction of **3****

enzyme	isomerization ^a		reduction ^b
	[2] in mM (relative activity ^c %)	ee of 2 (%)	conv (%)
GsOYE	8.21 (100)	79	>99
GsOYE-N270R	2.17 (26)	71	93
GsOYE-Y346F	5.95 (72)	59	94
GsOYE-Y179F	0.38 (5)	32	19
GsOYE-Y66F	0.17 (2)	65	96

^aReaction conditions: 10 mM **1**, 400 μ g/mL enzyme (\sim 10 μ M), Tris buffer (50 mM, pH 7), 2 vol % DMSO, 30 °C, 5 h. ^bReaction conditions: 10 mM **3**, 200 μ g/mL enzyme (\sim 5 μ M), 15 mM NADH, Tris buffer (50 mM, pH 7), 2 vol % DMSO, 30 °C, overnight. ^cWild-type activity set to 100%.

Scheme 3. Proposed Mechanism for the Isomerization of 1 to A) (*R*)-2 by GsOYE and B) (*S*)-2 by BfOYE4 Based on the Mutation Study, Crystal Structures, and Soaking Experiments



running the reaction at a lower pH value (7.5) with the wild-type strongly affected the extent of isomerization (max. 9% consumption at pH 7.5). Since both basic pH and availability of the tyrosine appear crucial for the reverse isomerization of *rac*-2 (Table 2), it is suggested that this residue—likely present as tyrosinate at pH 9—is involved in the enantioselective step of the reaction by deprotonating the γ -C. With GsOYE, the two other tyrosine residues Tyr66 and Tyr346 do not appear to be involved in the reverse reaction since mutation to phenylalanine did not significantly affect the extent of the reaction. In the crystal structure of GsOYE obtained after 7 h of soaking, a distance of 2.6 Å was measured between the γ -C of (*R*)-2 and the oxygen of Tyr₁₇₉-OH (compared to 4.4 Å with that of Tyr₆₆-OH), indicating a very favorable position for proton abstraction by Tyr179.

The mechanism of the dehydrogenation catalyzed by OYE homologues (often observed in the context of a redox neutral

disproportionation),^{49–52} while distinct from that of the isomerization reaction, proceeds following two concerted steps in opposite direction compared to the reduction reaction: deprotonation at the α -C likely by the conserved tyrosine and hydride abstraction by FMN at the β -C, as postulated by Massey and colleagues.⁵⁰ In the isomerization mechanism, catalytic deprotonation at the α -C of 1 may not be necessary, taking into account that (i) binding of the substrate carbonyl increases the acidity of α -H and induces the formation of an enolate-type bound substrate,⁴⁶ (ii) the corresponding enolate would be stabilized as an aromatic furan-type intermediate, and (iii) slightly basic pH favors the reaction (see Supporting Information, Scheme S2A). Based on soaking data, the involvement of GsOYE-Tyr179 in the deprotonation of 1 at the α -C (first step in 1 \rightarrow 2) and the protonation of 2 at the α -C (second step in 2 \rightarrow 1), respectively, remains however possible (3.3 and 3.6 Å, respectively, measured between the

Table 4. Activity of BfOYE4 Variants Compared to the Wild-Type in Isomerization of 1 to (S)-2 and Reduction of 3

enzyme	isomerization ^a		reduction ^b
	[2] in mM (relative activity ^c %)	ee of 2 (%)	conv (%)
BfOYE4	5.31 (100)	99	>99
BfOYE4-C76A	4.27 (80)	93	>99
BfOYE4-C76T	5.73 (108)	>99	48
BfOYE4-Y78F	4.09 (77)	25	>99
BfOYE4-Y78F ^d	2.08 (39)	25	n.a. ⁱ
BfOYE4-Y78F ^e	4.30 (81)	21	n.a. ⁱ
BfOYE4-Y235F	n.d. ^h	n.a. ⁱ	25 ^g
BfOYE4-K157A	1.00 (19)	91 ^f	86 ^g

^aReaction conditions: 10 mM 1, 400 μg/mL enzyme (~10 μM), Tris buffer (50 mM, pH 8), 2 vol % DMSO, 30 °C, 5 h. ^bReaction conditions: 10 mM 3, 200 μg/mL enzyme (~5 μM), 15 mM NADH, Tris buffer (50 mM, pH 7), 2 vol % DMSO, 30 °C, overnight. ^cWild-type activity set to 100%. ^dpH 7. ^epH 9. ^fON. ^gpH 7.5. ^hn.d. not detected. ⁱn.a. not applicable.

oxygen of Tyr₁₇₉-OH and the α-C of 1 and the α-C of (R)-2, respectively).

3. CONCLUSIONS

We have disclosed two stereocomplementary biocatalysts⁵³ from two classes of the Old Yellow Enzyme family for the highly stereoselective asymmetric isomerization of the prochiral model substrate γ-methyl β,γ-butenolide (1). The enzymatic protocol provides access to both (R)- and (S)-enantiomers of γ-methyl α,β-butenolide 2 in high ee values without racemization issues under mild reaction conditions. This study highlights the crucial role of tyrosine residues in asymmetric proton transfer catalysis for the isomerization of nonactivated C=C bonds and underscores the major differences between two stereodivergent members of two distinct OYE classes. The identification and characterization of further stereoselective isomerases within the OYE family will likely contribute to a global understanding of this hydride-free C=C bond isomerization mechanism unique among flavin-dependent enzymes. Noteworthy, this mechanism complements existing cases of enzymatic acid–base catalysis for C=C bond isomerization, which typically resort to Asp, Glu, or Cys for proton transfer. Because most reported cases of isomerases found in nature transform substrates that are not prochiral, stereoselective biocatalytic isomerization protocols for C=C bonds are rare.³⁷ The discovery of stereoselective Bronsted acid catalysis in a family of flavin-dependent redox enzymes indicates that the catalytic tyrosine, important in reduction reactions, needs not to be coupled to a hydride-transfer step. Mechanistically different, squalene hopene cyclases are terpene cyclases that protonate C=C double bonds through a catalytic aspartic acid. The event generating a carbocation initiates the cyclization reaction, and the protonation step could be exploited for a range of stereoselective reactions with non-natural substrates through protein engineering.⁵⁴ Our work opens the door to further discoveries connected to catalytic promiscuity in the family of OYEs with an already rich catalytic repertoire. Finally, this biocatalytic tool provides an attractive way to transform biomass-derived α-angelica lactone into valuable enantiopure precursors that can be incorporated into larger synthetic schemes⁵⁵ toward increased value from biomass, away from low value bulk chemicals.⁵⁶ Investigations

of the substrate scope are currently ongoing in our laboratory in order to evaluate the potential of a biocatalytic OYE isomerization platform in synthesis.

■ ASSOCIATED CONTENT

Supporting Information

The Supporting Information is available free of charge at <https://pubs.acs.org/doi/10.1021/acscatal.2c01110>.

Experimental procedures for preparation of enzymes and crystallography study, including structures of proteins and soaking experiments along with details on procedures to carry out biotransformations and analysis of reactions (NMR, GC, optical rotation) (PDF)

■ AUTHOR INFORMATION

Corresponding Author

Mélanie Hall – *Institute of Chemistry and Field of Excellence BioHealth, University of Graz, Graz, Styria 8010, Austria;*
orcid.org/0000-0003-4539-1992; Email: melanie.hall@uni-graz.at

Authors

Marina S. Robescu – *Department of Biology, University of Padova, Padova, Province of Padova 35131, Italy*
 Laura Cendron – *Department of Biology, University of Padova, Padova, Province of Padova 35131, Italy*
 Arianna Bacchin – *Institute of Chemistry, University of Graz, Graz, Styria 8010, Austria*
 Karla Wagner – *Institute of Chemistry, University of Graz, Graz, Styria 8010, Austria*
 Tamara Reiter – *Institute of Chemistry, University of Graz, Graz, Styria 8010, Austria*
 Ignacy Janicki – *Department of Heteroorganic Chemistry, Centre of Molecular and Macromolecular Studies, Polish Academy of Sciences, Lodz, Lodz Province 90-001, Poland;*
orcid.org/0000-0003-4700-3834
 Kemal Merusic – *Institute of Chemistry, University of Graz, Graz, Styria 8010, Austria*
 Maximilian Illek – *Institute of Chemistry, University of Graz, Graz, Styria 8010, Austria*
 Matteo Aleotti – *Institute of Chemistry, University of Graz, Graz, Styria 8010, Austria;* orcid.org/0000-0002-6016-0175
 Elisabetta Bergantino – *Department of Biology, University of Padova, Padova, Province of Padova 35131, Italy*

Complete contact information is available at: <https://pubs.acs.org/10.1021/acscatal.2c01110>

Author Contributions

The manuscript was written through contributions of all authors. All authors have given approval to the final version of the manuscript.

Notes

The authors declare no competing financial interest.

■ ACKNOWLEDGMENTS

We thank Alessia Tonoli for excellent technical assistance. A.B. benefited for her traineeship in Graz from an Erasmus+ student mobility grant from the University of Padova. We thank Prof. Paul Tudzynski from Münster University for the kind gift of *Botryotinia fuckeliana* B05.10 genomic DNA. M.S.R. was supported by a Ph.D. grant from F.I.S.-Fabbrica

Italiana Sintetici S.p.A. (Alte di Montecchio Maggiore, Italy). The authors acknowledge financial support by the University of Graz.

REFERENCES

- (1) Khersonsky, O.; Tawfik, D. S. Enzyme Promiscuity: A Mechanistic and Evolutionary Perspective. *Annu. Rev. Biochem.* **2010**, *79*, 471–505.
- (2) O'Brien, P. J.; Herschlag, D. Catalytic promiscuity and the evolution of new enzymatic activities. *Chem. Biol.* **1999**, *6* (4), R91–R105.
- (3) Humble, M. S.; Berglund, P. Biocatalytic Promiscuity. *Eur. J. Org. Chem.* **2011**, *2011* (19), 3391–3401.
- (4) Kazlauskas, R. J. Enhancing catalytic promiscuity for biocatalysis. *Curr. Opin. Chem. Biol.* **2005**, *9* (2), 195–201.
- (5) Sandoval, B. A.; Hyster, T. K. Emerging strategies for expanding the toolbox of enzymes in biocatalysis. *Curr. Opin. Chem. Biol.* **2020**, *55*, 45–51.
- (6) Sheldon, R. A.; Brady, D. Broadening the Scope of Biocatalysis in Sustainable Organic Synthesis. *ChemSusChem* **2019**, *12* (13), 2859–2881.
- (7) Toogood, H. S.; Gardiner, J. M.; Scrutton, N. S. Biocatalytic Reductions and Chemical Versatility of the Old Yellow Enzyme Family of Flavoprotein Oxidoreductases. *ChemCatChem* **2010**, *2* (8), 892–914.
- (8) Toogood, H. S.; Scrutton, N. S. Discovery, Characterization, Engineering, and Applications of Ene-Reductases for Industrial Biocatalysis. *ACS Catal.* **2018**, *8* (4), 3532–3549.
- (9) Williams, R. E.; Bruce, N. C. 'New uses for an Old Enzyme' - the Old Yellow Enzyme family of flavoenzymes. *Microbiology* **2002**, *148*, 1607–1614.
- (10) Hall, M.; Yanto, Y.; Bommarius, A. S. 'Old Yellow Enzyme' family and Enoate Reductases: Asymmetric Reduction of C = C Bonds and Activity on Nitro Compounds. In *The Encyclopedia of Industrial Biotechnology: Bioprocess, Bioproduction, and Cell Technology*; Flickinger, M., Ed.; John Wiley & Sons, Inc.: New York, 2010; pp 2234–2247.
- (11) Heckenbichler, K.; Schweiger, A.; Brandner, L. A.; Binter, A.; Toplak, M.; Macheroux, P.; Gruber, K.; Breinbauer, R. Asymmetric Reductive Carbocyclization Using Engineered Ene Reductases. *Angew. Chem. Int. Ed* **2018**, *57* (24), 7240–7244.
- (12) Sandoval, B. A.; Meichan, A. J.; Hyster, T. K. Enantioselective Hydrogen Atom Transfer: Discovery of Catalytic Promiscuity in Flavin-Dependent 'Ene'-Reductases. *J. Am. Chem. Soc.* **2017**, *139* (33), 11313–11316.
- (13) Sandoval, B. A.; Kurtoic, S. I.; Chung, M. M.; Biegasiewicz, K. F.; Hyster, T. K. Photoenzymatic Catalysis Enables Radical-Mediated Ketone Reduction in Ene-Reductases. *Angew. Chem. Int. Ed* **2019**, *58* (26), 8714–8718.
- (14) Biegasiewicz, K. F.; Cooper, S. J.; Gao, X.; Oblinsky, D. G.; Kim, J. B.; Garfinkle, S. E.; Joyce, L. A.; Sandoval, B. A.; Scholes, G. D.; Hyster, T. K. Photoexcitation of flavoenzymes enables a stereoselective radical cyclization. *Science* **2019**, *364* (6446), 1166–1169.
- (15) Page, C. G.; Cooper, S. J.; DeHovitz, J. S.; Oblinsky, D. G.; Biegasiewicz, K. F.; Antropow, A. H.; Armbrust, K. W.; Ellis, J. M.; Hamann, L. G.; Horn, E. J.; Oberg, K. M.; Scholes, G. D.; Hyster, T. K. Quaternary Charge-Transfer Complex Enables Photoenzymatic Intermolecular Hydroalkylation of Olefins. *J. Am. Chem. Soc.* **2021**, *143* (1), 97–102.
- (16) Huang, X. Q.; Wang, B. J.; Wang, Y. J.; Jiang, G. D.; Feng, J. Q.; Zhao, H. M. Photoenzymatic enantioselective intermolecular radical hydroalkylation. *Nature* **2020**, *584* (7819), 69–74.
- (17) Turrini, N. G.; Eger, E.; Reiter, T. C.; Faber, K.; Hall, M. Sequential Enzymatic Conversion of alpha-Angelica Lactone to gamma-Valerolactone through Hydride-Independent C = C Bond Isomerization. *ChemSusChem* **2016**, *9* (24), 3393–3396.
- (18) Xue, L.; Talalay, P.; Mildvan, A. S. Studies of the mechanism of the delta-5,3-ketosteroid isomerase reaction by substrate, solvent, and combined kinetic deuterium-isotope effects on wild-type and mutant enzymes. *Biochemistry* **1990**, *29* (32), 7491–7500.
- (19) Velarde, M.; Macieira, S.; Hilberg, M.; Broker, G.; Tu, S.; Golding, B.; Pierik, A.; Buckel, W.; Messerschmidt, A. Crystal Structure and Putative Mechanism of 3-Methylitaconate-Delta-isomerase from *Eubacterium barkeri*. *J. Mol. Biol.* **2009**, *391* (3), 609–620.
- (20) Street, I. P.; Coffman, H. R.; Baker, J. A.; Poulter, C. D. Identification of Cys139 and Glu207 as catalytically important groups in the active site of isopentenyl diphosphate-dimethylallyl diphosphate isomerase. *Biochemistry* **1994**, *33* (14), 4212–4217.
- (21) Thibodeaux, C.; Liu, H. The type II isopentenyl Diphosphate:Dimethylallyl diphosphate isomerase (IDI-2): A model for acid/base chemistry in flavoenzyme catalysis. *Arch. Biochem. Biophys.* **2017**, *632*, 47–58.
- (22) Unno, H.; Yamashita, S.; Ikeda, Y.; Sekiguchi, S.; Yoshida, N.; Yoshimura, T.; Kusunoki, M.; Nakayama, T.; Nishino, T.; Hemmi, H. New Role of Flavin as a General Acid-Base Catalyst with No Redox Function in Type 2 Isopentenyl-diphosphate Isomerase. *J. Biol. Chem.* **2009**, *284* (14), 9160–9167.
- (23) Durchschein, K.; Wallner, S.; Macheroux, P.; Zangger, K.; Fabian, W. M. F.; Faber, K. Unusual C = C Bond Isomerization of an alpha,beta-Unsaturated gamma-Butyrolactone Catalysed by Flavoproteins from the Old Yellow Enzyme Family. *ChemBioChem* **2012**, *13* (16), 2346–2351.
- (24) Wu, Y. W.; Singh, R. P.; Deng, L. Asymmetric Olefin Isomerization of Butenolides via Proton Transfer Catalysis by an Organic Molecule. *J. Am. Chem. Soc.* **2011**, *133* (32), 12458–12461.
- (25) Lee, J.; Deng, L. Asymmetric Approach toward Chiral Cyclohex-2-enones from Anisoles via an Enantioselective Isomerization by a New Chiral Diamine Catalyst. *J. Am. Chem. Soc.* **2012**, *134* (44), 18209–18212.
- (26) Robescu, M. S.; Niero, M.; Hall, M.; Cendron, L.; Bergantino, E. Two new ene-reductases from photosynthetic extremophiles enlarge the panel of old yellow enzymes: CtOYE and GsOYE. *Appl. Microbiol. Biotechnol.* **2020**, *104* (5), 2051–2066.
- (27) Liavonchanka, A.; Hornung, E.; Feussner, I.; Rudolph, M. G. Structure and mechanism of the Propionibacterium acnes polyunsaturated fatty acid isomerase. *Proc. Natl. Acad. Sci. U. S. A* **2006**, *103* (8), 2576–2581.
- (28) Scholtissek, A.; Tischler, D.; Westphal, A. H.; van Berkel, W. J. H.; Paul, C. E. Old Yellow Enzyme-Catalysed Asymmetric Hydrogenation: Linking Family Roots with Improved Catalysis. *Catalysts* **2017**, *7* (5), 130.
- (29) Romagnolo, A.; Spina, F.; Brenna, E.; Crotti, M.; Parmeggiani, F.; Varese, G. C. Identification of fungal ene-reductase activity by means of a functional screening. *Fungal Biol.* **2015**, *119* (6), 487–493.
- (30) Nizam, S.; Verma, S.; Borah, N.; Gazara, R.; Verma, P. Comprehensive genome-wide analysis reveals different classes of enigmatic old yellow enzyme in fungi. *Sci. Rep* **2014**, *4*, 4013.
- (31) Pesic, M.; Fernandez-Fueyo, E.; Hollmann, F. Characterization of the Old Yellow Enzyme Homolog from *Bacillus subtilis* (YqjM). *Chemistryselect* **2017**, *2* (13), 3866–3871.
- (32) Chaparro-Riggers, J. F.; Rogers, T. A.; Vazquez-Figueroa, E.; Polizzi, K. M.; Bommarius, A. S. Comparison of three enoate reductases and their potential use for biotransformations. *Adv. Synth. Catal.* **2007**, *349* (8–9), 1521–1531.
- (33) Riedel, A.; Mehnert, M.; Paul, C. E.; Westphal, A. H.; van Berkel, W. J. H.; Tischler, D. Functional characterization and stability improvement of a 'thermophilic-like' ene-reductase from *Rhodococcus opacus* ICP. *Front. Microbiol.* **2015**, *6*, 01073.
- (34) Lithauer, S.; Gargiulo, S.; van Heerden, E.; Hollmann, F.; Opperman, D. J. Heterologous expression and characterization of the ene-reductases from *Deinococcus radiodurans* and *Ralstonia metalidurans*. *J. Mol. Catal. B: Enzym* **2014**, *99*, 89–95.
- (35) Al-Shaal, M. G.; Ciptonugroho, W.; Holzhauser, F. J.; Mensah, J. B.; Hausoul, P. J. C.; Palkovits, R. Catalytic upgrading of alpha-

angelica lactone to levulinic acid esters under mild conditions over heterogeneous catalysts. *Catal. Sci. Technol.* **2015**, *5* (12), 5168–5173.

(36) Cui, H.-L.; Huang, J.-R.; Lei, J.; Wang, Z.-F.; Chen, S.; Wu, L.; Chen, Y.-C. Direct Asymmetric Allylic Alkylation of Butenolides with Morita–Baylis–Hillman Carbonates. *Org. Lett.* **2010**, *12* (4), 720–723.

(37) Dastmalchi, M.; Chen, X.; Hagel, J.; Chang, L.; Chen, R.; Ramasamy, S.; Yeaman, S.; Facchini, P. Neopinone isomerase is involved in codeine and morphine biosynthesis in opium poppy. *Nat. Chem. Biol.* **2019**, *15* (4), 384–390.

(38) Li, X.; Krysiak-Baltyn, K.; Richards, L.; Jarrold, A.; Stevens, G. W.; Bowser, T.; Speight, R. E.; Gras, S. L. High-Efficiency Biocatalytic Conversion of Thebaine to Codeine. *ACS Omega* **2020**, *5* (16), 9339–9347.

(39) Gomez-Bombarelli, R.; Gonzalez-Perez, M.; Perez-Prior, M. T.; Calle, E.; Casado, J. Computational Study of the Acid Dissociation of Esters and Lactones. A Case Study of Diketene. *J. Org. Chem.* **2009**, *74* (14), 4943–4948.

(40) Gollwitzer, J.; Lenz, R.; Hampp, N.; Zenk, M. H. The Transformation of Neopinone to Codeinone in Morphine Biosynthesis Proceeds Nonenzymatically. *Tetrahedron Lett.* **1993**, *34* (36), 5703–5706.

(41) Xue, X. S.; Li, X.; Yu, A.; Yang, C.; Song, C.; Cheng, J. P. Mechanism and Selectivity of Bioinspired Cinchona Alkaloid Derivatives Catalyzed Asymmetric Olefin Isomerization: A Computational Study. *J. Am. Chem. Soc.* **2013**, *135* (20), 7462–7473.

(42) Poterala, M.; Borowiecki, P. From Waste to Value—Direct Utilization of α -Angelica Lactone as a Nonconventional Irreversible Acylating Agent in a Chromatography-Free Lipase-Catalyzed KR Approach toward sec-Alcohols. *ACS Sustain. Chem. Eng.* **2021**, *9* (30), 10276–10290.

(43) Liavonchanka, A.; Rudolph, M. G.; Tittmann, K.; Hamberg, M.; Feussner, I. On the Mechanism of a Polyunsaturated Fatty Acid Double Bond Isomerase from *Propionibacterium acnes*. *J. Biol. Chem.* **2009**, *284* (12), 8005–8012.

(44) *The PyMOL Molecular Graphics System*, Version 2.0; Schrödinger, LLC.

(45) Hall, M.; Stueckler, C.; Ehammer, H.; Pointner, E.; Oberdorfer, G.; Gruber, K.; Hauer, B.; Stuermer, R.; Kroutil, W.; Macheroux, P.; Faber, K. Asymmetric bioreduction of C = C bonds using enoate reductases OPR1, OPR3 and YqjM: Enzyme-based stereocontrol. *Adv. Synth. Catal.* **2008**, *350* (3), 411–418.

(46) Kohli, R. M.; Massey, V. The oxidative half-reaction of old yellow enzyme - The role of tyrosine 196. *J. Biol. Chem.* **1998**, *273* (49), 32763–32770.

(47) Glanowski, M.; Wójcik, P.; Prochner, M.; Borowski, T.; Lupa, D.; Mielczarek, P.; Oszejka, M.; Świderek, K.; Moliner, V.; Bojarski, A. J.; Szaleniec, M. Enzymatic Δ 1-Dehydrogenation of 3-Ketosteroids—Reconciliation of Kinetic Isotope Effects with the Reaction Mechanism. *ACS Catal.* **2021**, *11* (13), 8211–8225.

(48) Hall, M.; Stueckler, C.; Kroutil, W.; Macheroux, P.; Faber, K. Asymmetric bioreduction of activated alkenes using cloned 12-oxophytodienoate reductase isoenzymes OPR-1 and OPR-3 from *Lycopersicon esculentum* (Tomato): A striking change of stereoselectivity. *Angew. Chem. Int. Ed* **2007**, *46* (21), 3934–3937.

(49) Buckman, J.; Miller, S. M. Binding and reactivity of *Candida albicans* estrogen binding protein with steroid and other substrates. *Biochemistry* **1998**, *37* (40), 14326–14336.

(50) Kelly, P. P.; Lipscom, D.; Quinn, D. J.; Lemon, K.; Caswell, J.; Spratt, J.; Kosjek, B.; Truppo, M.; Moody, T. S. Ene Reductase Enzymes for the Aromatisation of Tetralones and Cyclohexenones to Naphthols and Phenols. *Adv. Synth. Catal.* **2016**, *358* (5), 731–736.

(51) Stueckler, C.; Reiter, T. C.; Baudendistel, N.; Faber, K. Nicotinamide-independent asymmetric bioreduction of C = C-bonds via disproportionation of enones catalyzed by enoate reductases. *Tetrahedron* **2010**, *66* (3), 663–667.

(52) Vaz, A. D. N.; Chakraborty, S.; Massey, V. Old Yellow Enzyme - Aromatization of Cyclic Enones and the Mechanism of a Novel Dismutation Reaction. *Biochemistry* **1995**, *34* (13), 4246–4256.

(53) Mugford, P. F.; Wagner, U. G.; Jiang, Y.; Faber, K.; Kazlauskas, R. J. Enantiocomplementary Enzymes: Classification, Molecular Basis for Their Enantiopreference, and Prospects for Mirror-Image Biotransformations. *Angew. Chem. Int. Ed* **2008**, *47* (46), 8782–8793.

(54) Hammer, S. C.; Marjanovic, A.; Dominicus, J. M.; Nestl, B. M.; Hauer, B. Squalene hopene cyclases are protonases for stereoselective Bronsted acid catalysis. *Nat. Chem. Biol.* **2015**, *11* (2), 121–126.

(55) Mao, B.; Fananas-Mastral, M.; Feringa, B. L. Catalytic Asymmetric Synthesis of Butenolides and Butyrolactones. *Chem. Rev.* **2017**, *117* (15), 10502–10566.

(56) Wang, X. J.; Hong, M. Lewis-Pair-Mediated Selective Dimerization and Polymerization of Lignocellulose-Based β -Angelica Lactone into Biofuel and Acrylic Bioplastic. *Angew. Chem. Int. Ed* **2020**, *59* (7), 2664–2668.

Recommended by ACS

Biocatalytic, Stereoselective Deuteration of α -Amino Acids and Methyl Esters

Stephanie W. Chun and Alison R. H. Narayan

JUNE 23, 2020
ACS CATALYSIS

READ 

AoiQ Catalyzes Geminal Dichlorination of 1,3-Diketone Natural Products

Mengting Liu, Yi Tang, *et al.*

MAY 06, 2021
JOURNAL OF THE AMERICAN CHEMICAL SOCIETY

READ 

A Synthetic Alternative to Canonical One-Carbon Metabolism

Madeleine Bouzon, Philippe Marlière, *et al.*

MAY 03, 2017
ACS SYNTHETIC BIOLOGY

READ 

Mechanistic Investigation of Isonitrile Formation Catalyzed by the Nonheme Iron/ α -KG-Dependent Decarboxylase (ScoE)

Hong Li and Yongjun Liu

FEBRUARY 03, 2020
ACS CATALYSIS

READ 

Get More Suggestions >